Wrist-Powered Partial Hand Prosthesis Using a Continuum Whiffle Tree Mechanism: A Case Study

Kai Xu, *Member, IEEE*, Huan Liu, *Student Member, IEEE*, Zhaoyu Zhang, and Xiangyang Zhu, *Member, IEEE*

***Abstract*— Among the advances in upper extremity prostheses in the past decades, only a small portion of the results were obtained for partial hand prostheses, possibly due to the highly diverse partial hand presentations and limited space for component integration. In an attempt to address these challenges, this paper presents the design, construction, installation, and experimental characterization of a wrist-powered partial hand prosthesis developed in Shanghai Jiao Tong University (hereafter referred to as the JTP hand), customized for a specific amputee. The JTP hand possesses: 1) a continuum whiffle tree mechanism to allow adaptive grasping; 2) a force-magnifying partial gear pair to enhance the power of the grip; and 3) a phalange-embedded disengageable ratchet to enable or disable backdrivability. Various grasps and gestures were formed using the JTP hand. The obtained results suggest that the proposed design might be a viable option for patients with transmetacarpal amputation.**

***Index Terms*— Continuum mechanism, differential mechanism, force magnification, partial hand prosthesis, whiffle tree mechanism.**

I. Introduction

AN EPIDEMIOLOGICAL study estimated that approximately 1.6 million persons with limb loss were living in the United States in 2005 [1]. The primary causes leading to amputations were dysvascular diseases (54%) and trauma (45%). Among the amputations that involved the upper extremity, approximately 92% of the cases were partial hand amputations. Contrarily, among the advances in upper extremity prostheses in the past decades, only a small fraction of the results were obtained for partial hand prostheses. Possible reasons for this discrepancy include at least the following two aspects [2]. First, partial hand presentations are anatomically highly diverse. Therefore, it is difficult to standardize and scale a design. Second, the available space for component integration is limited, which makes it challenging to apply the solutions from the state-of-the-art prosthetic hands and arms (e.g., the ones in [3]–[9]).

Partial hand amputations have different levels [10]: i) transphalangeal amputation with spared thumb and loss of one or multiple fingers (Type-I), ii) thenar amputation with partial or complete loss of thumb (Type-II), iii) transmetacarpal distal amputation with resection across palm (Type-III), and iv) transmetacarpal proximal amputation with resection near the wrist (Type-IV).

It follows that due to the vulnerability of the digits, partial hand amputations are much more common, and significantly outnumber total hand and arm amputations. However, only a relatively small number of partial hand prostheses have been developed.

Partial hand prostheses can be either passive or active [2]. Passive prostheses mainly include cosmetic fingers and opposition posts (or prehension posts) [10], [11]. The latter is a mitt-like support that attaches the prosthesis (the thumb or the fingers) to one's stump so that the amputee can form opposition to handle and grip simple tools. For example, the M-Thumb (Partial Hand Solutions LLC) is such a passive opposition post with adjustable thumb position and resistance. Active partial hand prostheses can be powered by the body or externally. Their usefulness depends on properly forming opposition with appropriate grip force, movement speed and opening width.

Body-powered partial hand prostheses can use the shoulder, wrist or finger.

- Shoulder-powered prostheses (e.g., the Robin Aids partial hand [12] and the Handi-Hook from Hosmer Dorrance Corp.) are now mostly obsolete due to the complicated harness and the unnatural shoulder movements required to activate the prostheses.
- Finger-powered prostheses include the Partial M-finger^{TM} (Partial Hand Solutions LLC), the X-finger^{TM} (Didrick Medical Inc.), the Naked Finger^{TM} (Naked Prosthetics)

Manuscript received July 10, 2016; revised March 29, 2017 and November 3, 2017; accepted January 8, 2018. Date of publication February 2, 2018; date of current version March 6, 2018. This work was supported in part by the National Natural Science Foundation of China under Grant 51435010, Grant 51722507, Grant 51375295, and Grant 91648103, and in part by the National Program on Key Basic Research Projects under Grant 2011CB013300. *(Corresponding author: Kai Xu.)*

K. Xu and X. Zhu are with the State Key Laboratory of Mechanical System and Vibration, Shanghai Jiao Tong University, Shanghai 200240, China (e-mail: k.xu@sjtu.edu.cn; mexyzhu@sjtu.edu.cn).

H. Liu and Z. Zhang are with the Laboratory of Robotics Innovation and Intervention, UM-SJTU Joint Institute, Shanghai Jiao Tong University, Shanghai 200240, China (e-mail: liuhuan_2013@sjtu.edu.cn; zhangzhaoyu@sjtu.edu.cn).

Digital Object Identifier 10.1109/TNSRE.2018.2800162

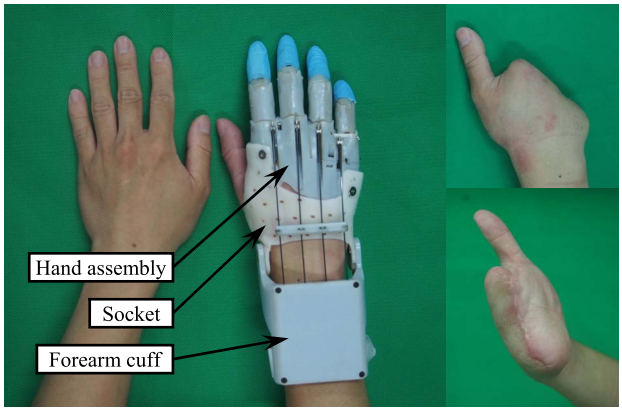

Fig. 1. The JTP hand worn by a partial hand amputee with presentation of the amputee's partial hand.

and the Knick Finger (a 3D printable finger design from the E-NABLE community). However, these designs can suffer from a lack of useable grip force.

- Wrist-powered prostheses include the pioneering design in [13] where a four-bar linkage was used to realize the wrist-driven open/close motions of the prosthetic hand. Linkage-based designs can also be found in [14] and [15] for different amputation conditions, and tendon actuation was shown to be effective in [16]. Commercial wrist-powered prostheses include the tendon-driven M-finger^{TM} (Partial Hand Solutions LLC), the linkage-based X-hand^{TM} (Didrick Medical Inc.), and various 3D printable hands from the E-NABLE community. The main disadvantages of the existing wrist-powered prostheses include i) constrained wrist movements for prostheses activation, ii) maintained wrist position for grip force preservation, and iii) plain cosmetic finishing.

Externally powered partial hand prostheses use miniature motors to drive the prosthetic fingers. The recent advances in mechatronics make these kinds of prostheses possible. Examples of these prostheses include designs [17]–[20] from academia. The first clinically available powered partial hand prosthesis is the ProDigits design from the Touch Bionics Inc. (formerly the Touch EMAS) [21]. Other commercially available powered partial hand prostheses include the Vincent Partial^{TM} from the Vincent Systems GmbH, the i-digits quantum^{TM} from the Touch Bionics Inc, etc. These motor-driven prostheses are usually non-backdrivable and controlled by signals from force sensitive resistors or electromyography (EMG). In theory these prostheses can form dexterous grasps and gestures but in reality their performances are often overshadowed by i) the relatively small grip force associated with the torque-magnifying transmission, ii) high cost stemmed from the system complexity, iii) prolonged hand control training, iv) limited battery life, etc.

After weighing the factors such as low output power from a miniature motor, low energy density of present battery, and the implementation challenges of EMG-based control, this paper presents the design, construction, installation, and experimental characterization of the JTP hand, a wrist-powered partial hand prosthesis, shown in Fig. 1, developed at Shanghai Jiao Tong University and customized for a specific amputee, as a case study. Aimed at improving the existing wrist-driven partial hand prostheses, the JTP hand possesses i) a continuum whiffle tree mechanism to allow adaptive grasping, ii) a force-magnifying partial gear pair to enhance the power of the grip, and iii) a disengageable phalange-embedded ratchet to enable or disable backdrivability. Experimental characterizations show that various grasps and gestures were formed using the JTP hand. The obtained results suggest that the proposed design may become a viable option for patients with transmetacarpal amputation.

This paper is organized as follows. With the design objectives and an overview of the JTP hand summarized in Section II, Section III describes the design process and the components of the JTP hand in detail. Section IV presents various experimental characterizations, and conclusions and future work are summarized in Section V.

II. Design Objectives and Overview

Normally the wrist is considerably stronger than a finger joint. Thus, the wrist is selected as the actuation source in order to achieve a higher grip force. The JTP hand was thus developed to provide prosthesis installation options for patients with transmetacarpal distal or transmetacarpal proximal amputations (Type-III or Type-IV as explained in Section I). Several design objectives were considered.

- Dimensions and kinematic structures of the JTP hand should allow the prosthesis to resemble the healthy side as similarly as possible. This resemblance concerns not only the dimensions and joint positions of the fingers but also their placements with respect to the stump.
- Total weight of the JTP hand should be less than 250 grams, which is about half the mass of a healthy adult's hand.
- There should be no protruding parts on the prosthetic hand to improve the cosmetic appearance.
- The fingers should be non-backdrivable so that the wrist does not need to maintain flexion to sustain the fingers' positions.
- The fingers could form adaptive grasps with enough grip forces.
- The fingers should be covered by materials with high friction for secure and stable grasps.
- Soft materials should be arranged inside the socket to improve the wearer's comfort.

The JTP hand, shown in Fig. 1, was then developed. The JTP hand consists of i) the partial hand assembly, ii) the socket, and iii) a forearm cuff with an integrated transmission module for differential outputs.

Two disengageable ratchets were embedded inside the distal phalanges of the index and the middle fingers to enable and disable backdrivability. A force-magnifying partial gear pair was integrated at the MCP (metacarpophalangeal) joints to enhance grip power. Efforts were made in the design process of the socket to ensure proper arrangement of the fingers. A continuum whiffle tree mechanism that has elastic links and no identifiable revolute joints was integrated inside the forearm cuff transmission module to allow the fingers to form

adaptive grasps. This mechanism was proposed as a two-stage continuum differential mechanism in [22] and [23]. Most of the existing wrist-driven partial hand prostheses directly connect the finger actuation strings to one spot in the forearm cuff. If these actuation strings are inextensible, when one or two strings are in tension, an amputee might not be able to continue to flex his/her wrist to close other fingers to form an adaptive grasp.

III. Design Descriptions

This section elaborates on the design process and component descriptions of the JTP hand. Section III.A describes the design approach used to ensure the prosthesis, once worn, would resemble the healthy hand as similarly as possible. Finger design optimization, ratchet integration and force magnifications are presented in Section III.B and Section III.C respectively. The continuum whiffle tree mechanism is explained in Section III.D to illustrate the design of the cuff-imbedded transmission module.

A. Finger Placement and Intended Fitting Process

The JTP hand, specifically customized for the amputee, was designed with a planned finger placement and intended stump fitting process. The goal was for the JTP hand, once worn, to resemble the other hand that is intact. The considerations presented here later become design constraints for several hand components as explained in later subsections.

Both the intact hand and the stump of the amputee were first digitized (scanned and imported into CAD software) as shown in Fig. 2(a). Then the intact hand was mirrored and overlaid on the stump as shown in Fig. 2(b). Since the stump was surgically formed, it was difficult to identify an exact match with the corresponding hand geometric features (e.g., around the hand heel). The overlay in Fig. 2(b) was obtained via careful observation. Then, the outer form of the partial hand assembly was obtained by subtracting the stump from the mirrored intact hand as shown in Fig. 2(c). It can be seen that the top of the stump is very close to the MCP (metacarpophalangeal) joint of the index finger. This caused fine adjustments in the structure of the force magnification mechanism.

All the hand components, as described in Section III.B and III.C, should be enveloped by the outer form of the partial hand assembly in Fig. 2(c). This envelopment has imposed a few design constraints on the linkages for the finger actuation.

It was decided to not activate the DIP (distal interphalangeal) joints to reduce the structural complexity. Then, the distal and the intermediate phalanges were used as-is from the scan. Locations of the PIP (proximal interphalangeal) and the MCP joints were estimated. The outer form of the partial hand was sliced and segmented to form the PIP and the MCP joints, as shown in Fig. 2(c). The lengths of the proximal phalanges are listed in Table I.

Even before the internal structure of the JTP hand was designed, a process that fits the partial hand to the amputee's stump was planned. Two matching holes were generated first

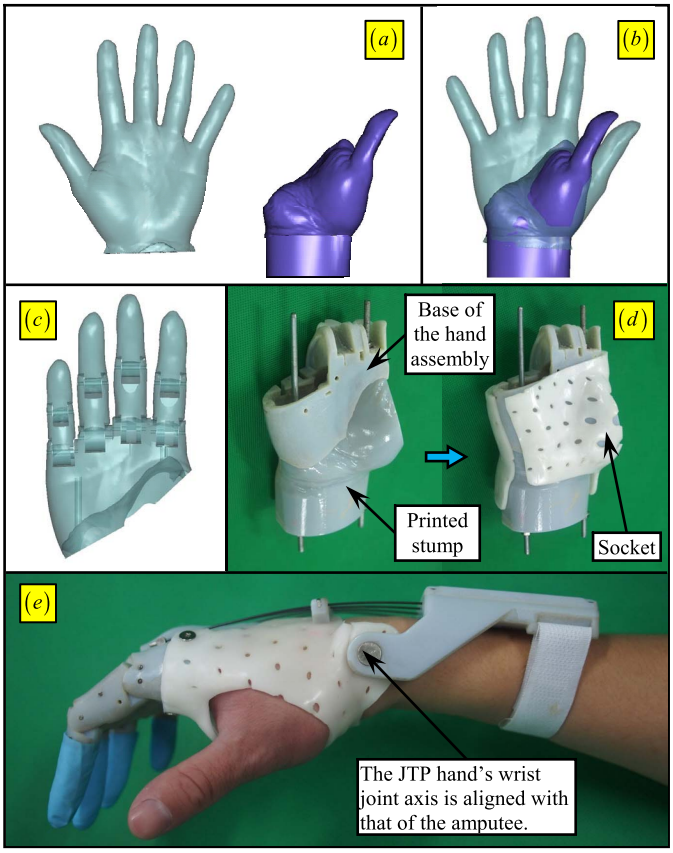

Fig. 2. Placement and fitting of the JTP hand: (a) the intact hand and the stump; (b) the intact hand is mirrored and overlaid on the stump; (c) the outer form of the JTP hand; (d) fitting the JTP hand to the stump; (e) determination of the wrist joint.

TABLE I
Structure Parameters of the JTP Hand

	Index	Middle	Ring	Little
Lengths of the proximal phalanges	28.0 mm	35.5 mm	31 .0 mm	22.5 mm

Parameters of the finger linkage	l_{OA}	l_{BC}	φ_1
Lower bound	4 mm	3 mm	45°
Upper bound	8 mm	6 mm	135°
Optimized value	4 mm	4 mm	50°

in the scanned stump and the outer form of the partial hand assembly. Then, the stump was printed and connected to the fabricated partial hand assembly with two pins inserted in the matching holes to fix the assembly precisely to the stump, as shown in the left image of Fig. 2(d). A thermoplastic board was heated and softened so that it could be closely wrapped around the partial hand assembly and the stump to form the socket, as shown in Fig. 2(d). The socket was cooled, rigidified and attached to the hand assembly using a few screws. Then, the printed stump was removed. When the socket is pried open and worn on the amputee's stump, the fingers and their joints are believed to be at positions close to the original positions of the lost half hand.

The JTP hand is powered by wrist flexion. It is also very important to align the rotary wrist joint axis of the JTP hand

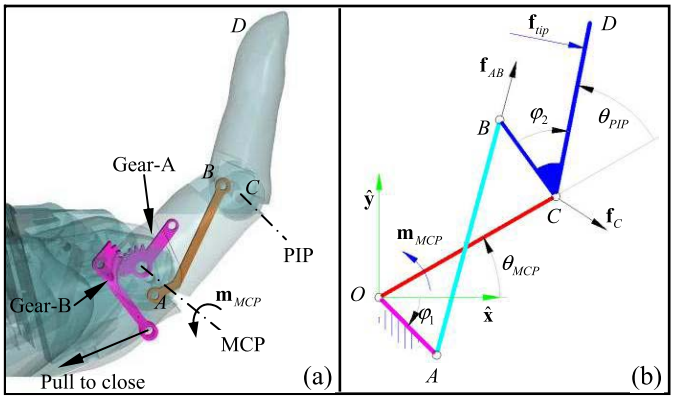

Fig. 3. Design of the index finger: (a) structural form and (b) schematic.

to the amputee's wrist joint. The places of the holes in the socket were only finalized when the JTP hand was worn by the amputee with a few trials of flexions and extensions, as shown in Fig. 2(e).

Through this carefully planned fitting procedure, the JTP hand is fully customized to the specific amputee. The partial hand, once worn, will resemble the other hand that is intact.

B. Design and Optimization of the Fingers

Since the wrist flexion is the only power source for the JTP hand, it was decided that the PIP joints should be coupled to the MCP joints. Then the input from the wrist flexion generates four differential outputs via the continuum whiffle tree mechanism in the forearm cuff to drive the four fingers.

The actuation scheme of the index finger is shown in Fig. 3.

As a nitinol (nickel-titanium super-elastic alloy) rod pulls Gear-B, a torque $\mathbf{m}_{MCP}$ is generated on the proximal phalange through the meshed Gear-A.

The coupling between the PIP joints and the MCP joints is realized by a crossed coupling. This mechanism is commonly used in prosthetic hand designs. Examples of prostheses that use this mechanism include the i-limb hand (Touch Bionics Inc.), the Vincent hand (Vincent Systems GmbH), the Bebionic hand (RSL Steeper), and the ones from academia (e.g., the SVEN hand [24], the Montreal Hand [25], the Robonaut hand [26], etc).

The schematic of the index finger, together with the structural parameters, is shown in Fig. 3(b). With an external force, $\mathbf{f}_{tip}$, assumed at the fingertip perpendicular to the distal phalange, the driving torque, $\mathbf{m}_{MCP}$, can be obtained through the formulation in (1), concerning the force and moment equilibrium of the proximal phalange (the OC link) and the intermediate-distal phalange (the BCD link).

$$\begin{cases} \mathbf{m}_{MCP} + \overrightarrow{OC} \times \mathbf{f}_C = \mathbf{0} \\ \overrightarrow{CB} \times \mathbf{f}_{AB} + \overrightarrow{CD} \times \mathbf{f}_{tip} = \mathbf{0} \\ \mathbf{f}_{AB} + \mathbf{f}_{AB} + (-\mathbf{f}_C) = \mathbf{0} \end{cases} \tag{1}$$

Where $\mathbf{f}_C$ is the force exerted on the OC link by the BCD link, and $\mathbf{f}_{AB}$ is the force exerted on the BCD link by the coupler (the AB link).

The structural parameters of the actuation linkage include the lengths and the angles to specify the position of the crossed coupler, namely, l_{OA}, l_{AB}, l_{BC}, φ_1 and φ_2. The lengths of the OC and the CD links are determined from the scan of the hand.

The parameters (l_{OA}, l_{AB}, l_{BC}, φ_1 and φ_2) should be optimized so that the fingers respond to the actuation in a desired way. Since the PIP joint is coupled to the MCP joint, the optimization is conducted towards a consistent linear mapping between the PIP and the MCP joints. Namely, in the desired case, θ_{MCP} is equal to θ_{PIP}. Then, the cost function can be formulated as follows, where θ_{PIP} is a function of θ_{MCP}.

$$\min \int_{\theta_{MCP}=0^\circ}^{\theta_{MCP}=90^\circ} \left(\theta_{PIP}\left(\theta_{MCP}\right) - \theta_{MCP}\right)^2 \tag{2}$$

The constraints to the optimization problem are formulated as in (3). These constraints require that the finger can be fully extended or clenched.

$$\begin{cases} \theta_{PIP} = 0^\circ, & \text{when } \theta_{MCP} = 0^\circ \\ \theta_{PIP} = 90^\circ, & \text{when } \theta_{MCP} = 90^\circ \end{cases} \tag{3}$$

The reason for formulating such an optimization is as follows. If the PIP joint is not approximately linearly coupled to the MCP joint, due to the constraint in (3), for the same amount of rotation in the MCP joint, the PIP joint would rotate more and then less (or vice versa). In this case, it would be more difficult for the amputee to produce subtle and well-controlled grasps. As the wrist flexion is directly related to the rotation of the MCP joints, a constant rotation speed in the MCP joints should not be accompanied with faster and then slower rotations in the PIP joints. Thus, the amputee is better able to achieve secure grasps no matter to what degree the fingers are extended or clenched. The optimization is not conducted towards a higher fingertip force, because a force magnifying mechanism, as presented in Section III.C was integrated to increase the grip force.

The optimization was conducted via enumeration of the free variables. Of the five parameters (l_{OA}, l_{AB}, l_{BC}, φ_1 and φ_2), only three are independent due to the two constraints listed in (3). When l_{OA}, l_{BC}, and φ_1 are enumerated, l_{AB} and φ_2 are first calculated using the two constraints in (3). The length of the proximal phalange (l_{OC}) is known. Then, the PIP joint angle (θ_{PIP}) is obtained for a given MCP joint angle (θ_{MCP}). In addition, the cost function in (2) is calculated with the θ_{MCP} discretized in increments of 5° from 0° to 90°.

The lower bounds, upper bounds and the final values of the parameters (l_{OA}, l_{BC}, and φ_1) are listed in Table I. In the enumeration, the lengths were discretized in increments of 0.1 mm with the angle discretized in increments of 5°. The lower and the upper bounds were decided primarily to ensure the links are all enveloped by the outer form of the finger. With the singular designs removed, the optimized values, listed in Table I, were obtained.

Using the optimized parameters, the rotation of the PIP joint with respect to the MCP joint is plotted in Fig. 4. The fingertip forces are also plotted, assuming 1 Nm actuation torque at the

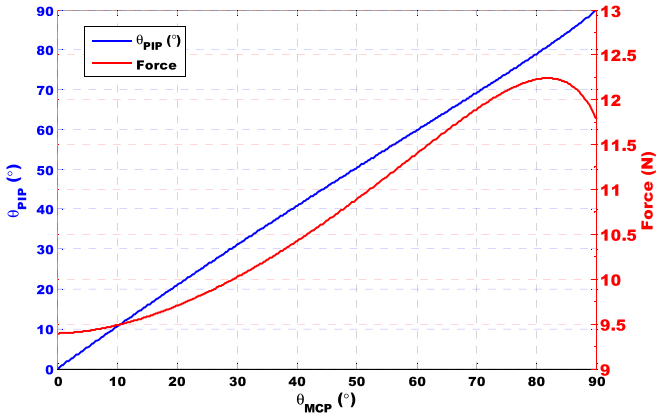

Fig. 4. PIP joint rotation and fingertip force plotted with respect to the MCP joint angle.

MCP joints. From the results in Fig. 4, it can be seen that the PIP joint rotates almost linearly with the MCP joint.

The optimization results of the index finger were also used for the middle, the ring and the little fingers. The rotations of the PIP joints and the fingertip forces with respect to the MCP joint rotations are similar to the results shown in Fig. 4.

C. Disengageable Ratchet and Grip Force Magnification

The PIP joint is coupled to the MCP joint and the MCP joint is actuated to close the finger to form grasps. Since the finger is thin relative to the palm, a half gear pair was implemented to make full use of the palm thickness, generating bigger driving torque for the MCP joint with the same pulling force from the actuation line.

As shown in Fig. 5, Gear-A is attached to the proximal phalange with a pitch diameter of 9.5 mm. Gear-B has a pitch diameter of 10.5 mm. Both gears have a module of 0.5 mm. The arm, extended from Gear-B, has a length of 20 mm. The Gear-A was made smaller to limit the rotating range of Gear-B so that the 20 mm arm does not interfere with the stump.

Gear-B's arm is pulled by the actuation line, which is a nitinol (nickel-titanium super-elastic alloy) rod from the continuum whiffle tree mechanism inside the forearm cuff. The connection between the arm and the actuation rod is only one-way. Thus, one end of the rod can be pushed out from the revolute pin joint, as shown in the upper inset of Fig. 5(a). This feature prevents excessive compressive forces from being exerted on the actuation rods when the fingers are accidentally pushed close.

Since the wrist flexes to actuate the JTP hand, it is highly desired that the fingers could be non-backdrivable or lockable so that grasps or gestures could be maintained without requiring continuous flexion forces from the wrist.

With the coupler and the gear inside the proximal phalange, the distal and the intermediate phalanges are used to house the switching mechanism to engage or disengage a ratchet. The ratchet is fixedly attached to the intermediate phalange. The pawl is spring-loaded for constant engagement. A rod that protrudes from the switching mechanism pushes the pawl to disengage the ratchet. While the ratchet is engaged, the PIP

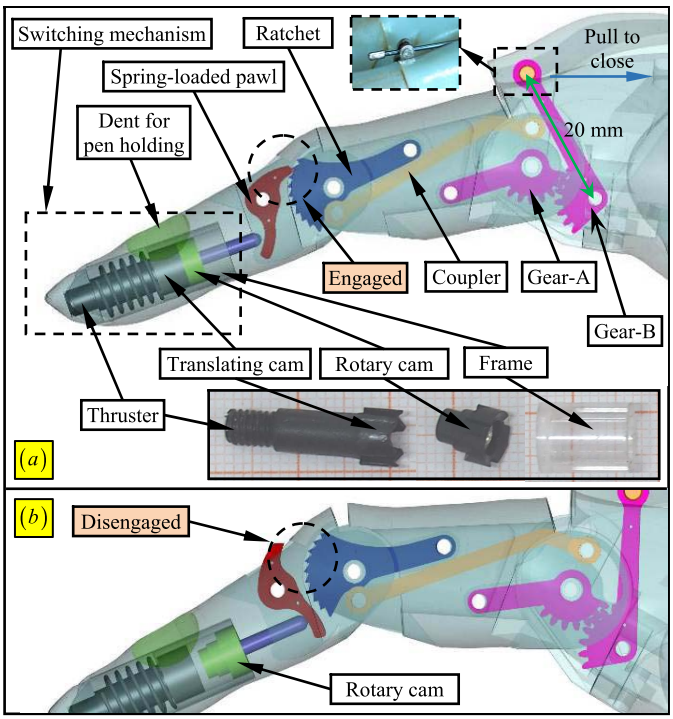

Fig. 5. The disengageable ratchet and the gear pair for force magnification: the ratchet (a) engaged and (b) disengaged.

and the MCP joints become non-backdrivable (the finger could not be pried open). Once disengaged, the joints rotate freely.

The switching mechanism was cut from a retractable pen. The design is patented by Parker Pen Co. [27]. The design consists of a frame, a thruster, a translating cam, a rotary cam and a spring. The rod is connected with the rotary cam. The two cams form a two-configuration system where in one position, the rod is retracted and in the other, the rod is extended.

The thruster is connected with the fingertip. Clicked once, the rod extends to disengage the ratchet. Clicked again, the rod retracts and the pawl engages the ratchet.

A dent was produced on the phalange surface for holding a pen to facilitate writing using the JTP hand, as shown in Section IV.C.

D. Continuum Whiffle Tree Mechanism

The continuum whiffle tree mechanism was addressed as a continuum differential mechanism in [22] and [23]. This mechanism is a new type of differential mechanism that generates differential outputs via structural deformations. The working principle is explained as in Fig. 6(a).

The general basic form of the continuum differential mechanism consists of a base link, an end link, an input and two output backbones. All the backbones are made from super-elastic nitinol. They are attached to the end link and can slide in holes in the base link. A force, f_a, acts on the central backbone as the input so that two outputs push two external objects. When the load on the left is bigger, continuously driving the input backbone bends all the backbones to generate differential outputs. Then, the object on the right is pushed

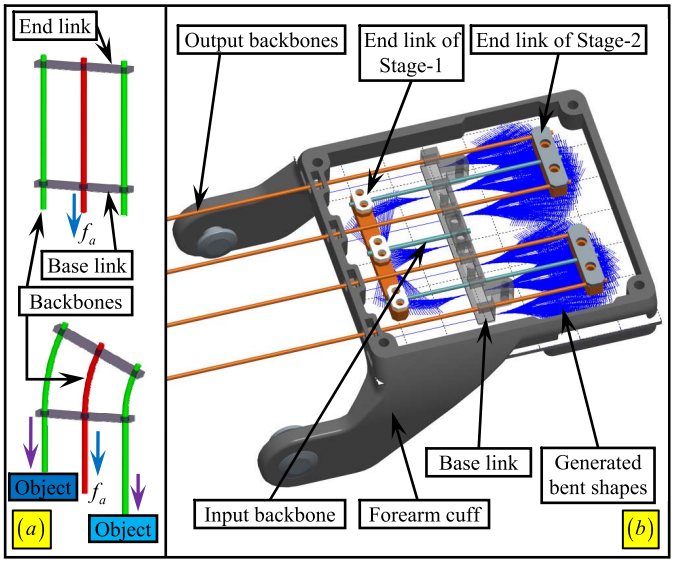

Fig. 6. Continuum whiffle tree mechanism: (a) a general basic form, and (b) implementation in the forearm cuff of the JTP hand.

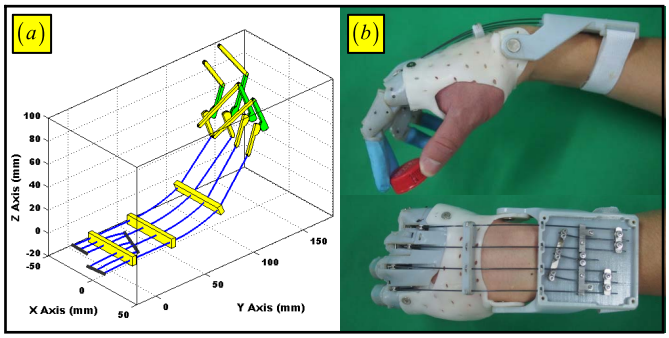

Fig. 7. Bent statuses of the continuum whiffle tree mechanism: (a) a Matlab simulation, (b) under an actual pinch pose.

further. The continuum differential mechanism could provide pushing and pulling outputs, since the backbones can be pushed or pulled.

On the other hand, the whiffle tree mechanism is an ancient device used in numerous mechanical applications for centuries. The use of this mechanism in prosthetic hands can be traced back to 1910s [28]. Later hand designs with the whiffle tree mechanism in its traditional form include the ones in [29]–[31].

The presented continuum whiffle tree mechanism does not have identifiable revolute joints. It is advantageous in terms of structural simplicity, design compactness and light weight. Due to the backbones' intrinsic elasticity, it does not require any tension-keeping components. And the mechanism's intrinsic elasticity will always restore it to the original pose.

The wrist flexion drives four fingers. Hence, the continuum whiffle tree mechanism integrated inside the forearm cuff has two stages, leading to four outputs, as shown in Fig. 6(b). The base link is attached to the forearm cuff. An input backbone is attached to both the base link and Stage-1's end link. When the forearm cuff is rotated during wrist flexion, attaching the input backbone to the base link is equivalent to pulling the input backbone if the forearm cuff were stationary. Two output backbones of Stage-1 act as the inputs backbones of Stage-2. Thus, four outputs are generated.

Detailed modeling and analysis of the continuum differential mechanism can be found in [23], where the bent backbones are modeled as circular arcs.

In the presented design, all the backbones are Ø1 mm nitinol rods. The distance between the four output backbones is 15 mm. This was determined according to the finger separation and palm width of the amputee. Then, the width of the Stage-1 and Stage-2 structure can be determined by evenly distributing the backbones.

The output backbone is pulled for approximately 20 mm to fully close a finger. When an adaptive grasp is formed for an object, the output backbones are pulled differently so that the fingers are closed adaptively. Different pulling lengths on the output backbones correspond to different bent shapes of the continuum whiffle tree mechanism. The lengths of the Stage-1 and the Stage-2 structures are checked to verify two aspects. First, the forearm cuff should be big enough to house the mechanism. Second, the biggest strain on the backbone should be kept below the allowed limit for elastic deformations when they are bent. The elastic strain of super-elastic nitinol ranges from 4% to 6%. A 3% strain limit was used here.

The length of the Stage-1 structure was set to 20 mm, while that of Stage-2 was 25 mm. The lengths were enumerated from the possible values with increments of 5 mm. Then, the bent shapes of the continuum whiffle tree mechanisms were generated when the output backbones were pulled differently from 0 mm to 20 mm. A simulated hand pose is plotted in Fig. 7(a), while an actual bent shape of the mechanism is shown in Fig. 7(b) under a pinch pose for a bottle cap.

When the bent shapes of the mechanism are generated, one constraint was used as follows. The difference in the pulling lengths between adjacent output backbones should be equal to or smaller than 10 mm. Without this constraint, the mechanism would be considerably longer and the forearm cuff would be unnecessarily big, simply to include the hand poses that do not often occur in daily activities.

The generated bent shapes were overlaid on the forearm cuff as shown in Fig. 6(b) to ensure the cuff is big enough to house the continuum whiffle tree mechanism.

IV. Experimental Characterizations

The JTP hand was mostly fabricated with 3D printing. Critical transmission and actuation components were made from stainless steel. Silicone rubber was placed between the partial hand assembly and the stump inside the socket to improve the wearing comfort. Its total weight is 245 grams.

Then the JTP was worn by an amputee and a series of experiments were conducted to demonstrate the effectiveness and usefulness of the JTP hand. The amputee is a 33-year-old male who underwent transmetacarpal amputation on his right hand in August 2015. The amputation resulted from a work injury. Prior to the injury, the amputee was right-handed. Before this research, he primarily used a cosmetic

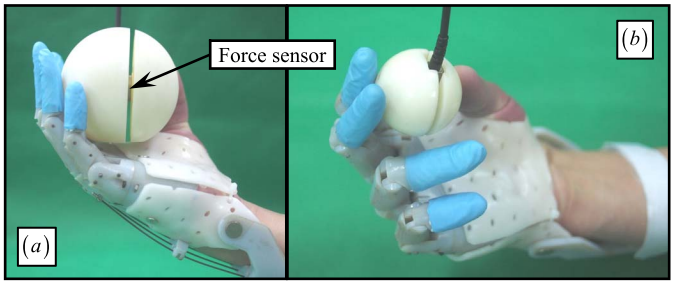

Fig. 8. The experimental setting for (a) grasp and (b) pinch force measurements.

TABLE II
FORCES MEASURED FROM POWER GRASP AND PINCH

Power grasp			
Trials	1st	2nd	3rd
X component from the sensor	-2.52 N	0.87 N	-0.81 N
Y component from the sensor	1.87 N	-8.45 N	-6.46 N
Z component from the sensor	-13.91 N	-11.94 N	-16.36 N
Norm of the force	14.26 M	14.65 N	17.60 N
Average force	15.50 N		
Pinch			
Trials	1st	2nd	3rd
X component from the sensor	2.01 N	0.32 N	0.89 N
Y component from the sensor	0.31 N	-2.66 N	0.33 N
Z component from the sensor	-7.21 N	-9.54 N	-8.62 N
Norm of the force	7.49 N	9.91 N	8.67 N
Average force	8.69 N		

hand prosthesis and a simple opposition post. He has no experience with any active prosthesis.

A. Grip and Pinch Forces

It is paramount that the JTP hand can generate enough forces for various grasps and pinches. The force quantification was conducted first, as follows.

As shown in Fig. 8(a), one force sensor (Nano 17 for six dimensional measurements from ATI Inc.) was installed inside a ball with a diameter of 73 mm. The ball that is at the size of a baseball was 3D printed as two pieces and assembled to both mounting surfaces of the force sensor. The amputee was asked to flex his wrist as hard as he could three times. The results are listed in Table II.

The pinch experiment was conducted as shown in Fig. 8(b). The Nano 17 force sensor was installed inside a 3D-printed smaller ball with a diameter of 40 mm. The ball was placed at the fingertips of the amputee, and the amputee was asked to pinch as hard as he could three times. The pinching force results are also listed in Table II.

Average forces of 15.5 N and 8.69 N for the power grasp and pinch respectively are considered well acceptable for most daily life activities.

B. Hand Function Assessment

Wearing the JTP hand, the amputee performed grasps and pinches easily with his wrist flexed. Depending on the objects

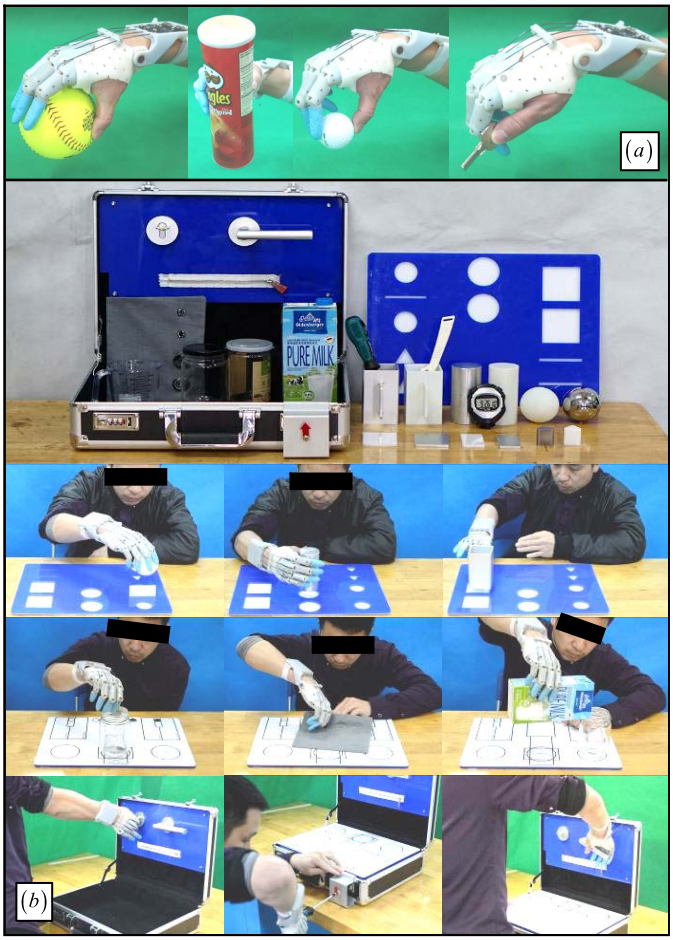

Fig. 9. Function demonstrations: (a) grasps and pinches, and (b) the SHAP test.

to be grasped or pinched, the wrist should flex in a range from 10° to 40°. The outputs from the continuum whiffle tree mechanism in the forearm cuff varied to form adaptive grasps and natural-looking pinch poses, as shown in Fig. 9(a). To increase friction during grasps and pinches, the finger portions of a latex house-keeping glove were cut off and put on the fingers of the JTP hand. Some of the objects grasped are from the YCB object set [32].

It was desired that the function of the JTP hand could be systematically examined. To evaluate the functions of hand prostheses, several measures have been established according to a comprehensive survey and an initiative to unify such measures [33], [34]. Due to the availability of the testing kit, the Southampton Hand Assessment Procedure (SHAP) [35] was followed in this study.

A SHAP kit was obtained as shown in Fig. 9(b). The amputee was asked to perform two sets of tasks using the JTP hand, following the SHAP test protocol. The SHAP test is considered to provide quantitative and objective assessment.

The first set of tasks in the SHAP test is to grasp and place 12 abstract objects from and to designated positions, sometimes over an obstacle. The 12 abstract objects are 6 light and 6 heavy objects with the identical shapes of i) sphere, ii) small triangular prism, iii) thick cylinder, iv) rectangular tube with handle, v) thin strip, and vi) thin plate.

TABLE III
IOF AND FP SCORES FOR THE JPT HAND AND THE VMG HAND IN [36]

	IoF Index	Functionality Profile (FP)						FP Mean	FP Std Dev
		Pow.	Sph.	Ext.	Trip.	Lat.	Tip		
VMG hand [36]	**87**	85	90	90	82	89	78	86	4.9
JTP hand	**83**	90	86	84	86	72	88	84	6.3

The second set of tasks is to perform Activities of Daily Living (ADLs), including i) picking up coins and putting them into a jar, ii) undoing buttons, iii) cutting food, iv) picking up and flipping a piece of paper, v) opening a jar, vi) pouring water from a jug by holding the handle, vii) holding and pouring milk from a carton, viii) picking up and placing a jar with half-filled water, ix) picking up and placing a plate, x) turning a key, xi) pulling a zipper, xii) using a screwdriver, and xiii) turning a door handle.

With the JTP hand, the amputee was able to perform all the SHAP tasks after using the prosthesis for a few hours. Representative grasps and motions during the test are shown in Fig. 9(b). His quick adaption could be partially due to the previous training he received from an occupational therapist on how to use a cosmetic prosthetic hand and a simple opposition post.

The SHAP test provides an Index of Function (IoF) score to measure hand function. A healthy subject usually has an IoF score from 95 to 100. Lower IoF indicates severer impairment.

The time needed to finish each task in the SHAP test is first used to calculate Functionality Profile (FP) scores for the power, spherical, extension, tripod, lateral and tip grasps. Then, the IoF scores are obtained from the FP scores. Details on determining the scores can be found in [35]. The IoF and FP scores for the amputee with the JTP hand are listed in Table III.

The scores for the VMG (Vanderbilt Multi-grasp) hand from [36] are also listed in Table III for comparison. The scores are higher, possibly because the VMG hand has nine DoFs (Degrees of Freedom) driven by four servomotors under myoelectric control. After the transradial amputee participated in four training sessions spanning several weeks, it is understandable that the use of the VMG hand leads to a higher IoF score than the JTP hand, which is purely mechanical and driven by wrist flexion.

A multi-media extension is included to show the grasps, pinches and the SHAP test procedure using the JTP hand.

Although the JTP hand is driven by wrist flexion, the pronation/supination of the wrist is still fully available. In the assessment, it was observed that the wrist's flexion for the actuation of the JTP hand did not result in awkward poses of the torso or the arm. Apparently the amputee did not need to compensate for the wrist's constrained movements.

The amputee failed to grasp objects with diameters bigger than about two thirds of the maximal opening width of the thumb-JTP hand (namely, the width of the oblique arches). Due to the small size of the amputee's original hand, he could only grasp a soft ball (with a diameter of 96.5 mm) with the JTP hand, as shown in Fig. 9(a). For bigger balls, it was difficult for him to achieve a stable grasp. The reasons include primarily two aspects: i) the DIP joints are fixed, and ii) the PIP and the MCP joints are coupled. Ejection in grasps could occur if the object to be grasped is too big.

Fig. 10. Gestures and functions using the lockable fingers: (a) writing, (b) typing, (c) weight (2kg) hanging, (d) mug holding, and (e) posing for okay.

The wrist needs to flex up to 40° to pinch small objects (e.g. the two-finger pinch for a key). This creates a level of discomfort due to the imperfect design of the socket. The current socket fabrication emphasizes conformity to the stump too much, and might have overlooked leaving enough room for the stump to deform during wrist motions.

C. Lockable Fingers

The index and the middle fingers could be locked so that they become non-backdrivable. Then, the amputee can maintain grasps without keeping the wrist flexion/extension positions. Namely, the grasps are formed by the thumb and the locked index and/or middle fingers; the wrist is free to move under this condition.

This feature allowed the JTP hand to form unique postures to further expand its functions and uses, besides adaptive grasps and pinches.

As shown in Fig. 10(a), the intact hand could close the index and the middle fingers of the JTP hand to suitable angles so that a pen could be held with the thumb. Dents were created on the surfaces of the index and the middle fingers to facilitate pen holding. Then, the amputee was able to write.

The index finger could be locked at different angles so that the amputee could perform keyboard striking and posing for okay easily, as shown in Fig. 10(b) and Fig. 10(e). With the index and the middle fingers locked, he could also hold a mug with ease, as shown in Fig. 10(d).

The lockable fingers are particularly useful in the scenario of weight hanging. As shown in Fig. 10(c), the two locked fingers could bear a weight of 2 kg (approximately 4 pounds). The extreme loading capacity was not tested because the JTP hand can easily be made stronger using industry-grade plastics, instead of thermoplastics from a 3D printer. While the weight and cost would be increased with the use of better plastics, design decisions will be made to balance these contradicting aspects.

The weight hanging was not conducted when the JTP hand was worn by the amputee. Due to the imperfect design of the socket, the socket hurts the thumb near the thumb's metacarpal area, when the weight was too heavy. Improvement on the socket fabrication is in due course.

V. Conclusion and Future Work

This paper reports the design, construction, installation, and experimental characterizations of a wrist-powered, customized partial hand prosthesis, referred to as the JTP hand, developed at Shanghai Jiao Tong University. This development aims at providing one viable prosthesis option for transmetacarpal partial hand amputees.

Three main features were integrated into the JTP hand: i) a continuum whiffle tree mechanism for adaptive grasps, ii) a force-magnifying partial gear pair for enhanced grip and pinch forces, and iii) a phalange-embedded disengageable ratchet to enable or disable backdrivability. It has been demonstrated that various grasps, pinches and gestures can be formed using the JTP hand, indicating the practical value of this design.

A few improvements are expected to be included in the near future. Passive distal interphalangeal joints are planned so that it is easier for an amputee to grasp large objects using the new JTP hand. Structural modifications need to be introduced to transform the current continuum whiffle tree mechanism into a layered configuration so that the size of the forearm cuff can be reduced. The socket design should be substantially improved to increase the comfort while wearing the JTP hand. In addition, it is also desired to make the JTP hand lighter (e.g., below 200 grams) and stronger by trimming the internal structures and using plastics components made from injection molding.

Acknowledgment

The authors appreciate the advices and suggestions from the anonymous reviewers for improving the quality of this manuscript.

References

[1] K. Ziegler-Graham, E. J. MacKenzie, P. L. Ephraim, T. G. Travison, and R. Brookmeyer, "Estimating the prevalence of limb loss in the United States: 2005 to 2050," *Archi. Phys. Med. Rehabil.*, vol. 89, no. 3, pp. 422–429, 2008.

[2] I. Imbinto *et al.*, "Treatment of the partial hand amputation: An engineering perspective," *IEEE Rev. Biomed. Eng.*, vol. 9, pp. 32–48, 2016.

[3] H. Kawasaki, T. Komatsu, and K. Uchiyama, "Dexterous anthropomorphic robot hand with distributed tactile sensor: Gifu hand II," *IEEE/ASME Trans. Mechatronics*, vol. 7, no. 3, pp. 296–303, Sep. 2002.

[4] J. W. Sensinger and R. F. F. Weir, "User-modulated impedance control of a prosthetic elbow in unconstrained, perturbed motion," *IEEE Trans. Biomed. Eng.*, vol. 55, no. 3, pp. 1043–1055, Mar. 2008.

[5] S. A. Dalley, T. E. Wiste, T. J. Withrow, and M. Goldfarb, "Design of a multifunctional anthropomorphic prosthetic hand with extrinsic actuation," *IEEE/ASME Trans. Mechatronics*, vol. 14, no. 6, pp. 699–706, Dec. 2009.

[6] M. Grebenstein *et al.*, "The hand of the DLR hand arm system: Designed for interaction," *Int. J. Robot. Res.*, vol. 31, no. 13, pp. 1531–1555, 2012.

[7] J. T. Belter, J. L. Segil, A. M. Dollar, and R. F. Weir, "Mechanical design and performance specifications of anthropomorphic prosthetic hands: A review," *J. Rehabil. Res. Develop.*, vol. 50, no. 5, pp. 599–618, 2013.

[8] G. Palli *et al.*, "The DEXMART hand: Mechatronic design and experimental evaluation of synergy-based control for human-like grasping," *Int. J. Robot. Res.*, vol. 33, no. 5, pp. 799–824, Apr. 2014.

[9] M. G. Catalano, G. Grioli, E. Farnioli, A. Serio, C. Piazza, and A. Bicchi, "Adaptive synergies for the design and control of the pisa/IIT SoftHand," *Int. J. Robot. Res.*, vol. 33, no. 5, pp. 768–782, Apr. 2014.

[10] L. F. Bender, "Prostheses for partial hand amputations," *Prosthetics Orthotics Int.*, vol. 2, no. 1, pp. 8–11, 1978.

[11] W. S. Dewey *et al.*, "Opposition splint for partial thumb amputation: A case study measuring disability before and after splint use," *J. Hand Therapy*, vol. 22, no. 1, pp. 79–87, 2009.

[12] R. Anderson, "How to fit the robin-aids partial hand," UCLA Prosthetics Education Program, Los Angeles, CA, USA, Tech. Rep., 1961.

[13] G. Rubin, M. Danisi, and E. Lamberty, "A wrist driven hand prosthesis," *Bull. Prosthetics Res.*, vol. 10, no. 18, pp. 40–45, 1973.

[14] T. Dick, D. W. Lamb, and W. B. Douglas, "A wrist-powered hand prosthesis," *J. Bone Joint Surg.*, vol. 66, no. 5, pp. 742–744, 1984.

[15] J.-H. Shim, Y.-H. Lee, J.-M. Lee, J. M. Park, and J.-H. Moon, "Wrist-driven prehension prosthesis for amputee patients with disarticulation of the thumb and index finger," *Arch. Phys. Med. Rehabil.*, vol. 79, no. 7, pp. 877–878, 1998.

[16] D. P. Cole, G. L. Davis, and J. E. Traunero, "The toledo tenodesis prosthesis—A case history utilizing a new concept in prosthetics for the partial hand amputee," *Orthotics Prosthetics*, vol. 38, no. 4, pp. 13–23, 1985.

[17] R. F. Weir, E. C. Grahn, and S. J. Duff, "A new externally powered, myoelectrically controlled prosthesis for persons with partial-hand amputations at the metacarpals," *J. Prosthetics Orthotics*, vol. 13, no. 2, pp. 26–31, 2001.

[18] C. Lake, "Experience with electric prostheses for the partial hand presentation: An eight-year retrospective," *J. Prosthetics Orthotics*, vol. 21, no. 2, pp. 125–130, Apr. 2009.

[19] J. E. Uellendahl and E. N. Uellendahl, "Experience fitting partial hand prostheses with externally powered fingers," in *Grasping the Future: Advances in Powered Upper Limb Prosthetics*, V. P. Castelli and M. Troncossi, Eds. Sharjah, United Arab Emirates: Bentham Science Publishers, 2012, pp. 15–27.

[20] S. Schulz, "Finger Element," U.S. Patent 8 491 666, Jul. 23, 2013.

[21] D. J. Gow, *Prostheses With Mechanically Operable Digit Members*. Livingston, U.K.: Touch Emas Limited, 2009.

[22] K. Xu, H. Liu, Z. Liu, Y. Du, and X. Zhu, "A single-actuator prosthetic hand using a continuum differential mechanism," in *Proc. IEEE Int. Conf. Robot. Autom. (ICRA)*, Seattle, WA, USA, May 2015, pp. 6457–6462.

[23] K. Xu and H. Liu, "Continuum differential mechanisms and their applications in gripper designs," *IEEE Trans. Robot.*, vol. 32, no. 3, pp. 754–762, Jun. 2016.

[24] C. Almström, P. Herberts, and L. Körner, "Experience with swedish multifunctional prosthetic hands controlled by pattern recognition of multiple myoelectric signals," *Int. Orthopaedics*, vol. 5, no. 1, pp. 15–21, 1981.

[25] R. Vinet, Y. Lozac h, N. Beaudry, and G. Drouin, "Design methodology for a multifunctional hand prothesis," *J. Rehabil. Res. Develop.*, vol. 32, no. 4, pp. 316–324, Nov. 1995.

[26] C. S. Lovchik and M. A. Diftler, "The robonaut hand: A dexterous robot hand for space," in *Proc. IEEE Int. Conf. Robot. Autom. (ICRA)*, Detroit, Michigan, May 1999, pp. 907–912.

[27] K. R. Nolan, *Writing Instrument*. Janesville, WI, USA: Parker Pen Co., 1965.

[28] M. Borchardt, K. Hartmann, R. Leymann, and S. Schlesinger, *Ersatzglieder und Arbeitshilfen für Kriegsbeschädigte und Unfallverletzte*. Berlin, Germany: Springer-Verlag, 1919.

[29] M. Rakić, "An automatic hand prosthesis," *Med. Electron. Biol. Eng.*, vol. 2, no. 1, pp. 47–55, Mar. 1964.

[30] N. Fukaya, S. Toyama, T. Asfour, and R. Dillmann, "Design of the TUAT/karlsruhe humanoid hand," in *Proc. IEEE/RSJ Int. Conf. Intell. Robots Syst. (IROS)*, Takamatsu, Japan, Oct./Nov. 2000, pp. 1754–1759.

[31] M. Baril, T. Laliberté, C. Gosselin, and F. Routhier, "On the design of a mechanically programmable underactuated anthropomorphic prosthetic gripper," *J. Mech. Des.*, vol. 135, no. 12, p. 121008-1, Oct. 2013.

[32] B. Calli, A. Walsman, A. Singh, S. Srinivasa, P. Abbeel, and A. M. Dollar, "Benchmarking in manipulation research: Using the yale-CMU-Berkeley object and model set," *IEEE Robot. Autom. Mag.*, vol. 22, no. 3, pp. 36–52, Sep. 2015.

[33] W. Hill, Ö. Stavdahl, L. N. Hermansson, P. Kyberd, S. Swanson, and S. Hubbard, "Functional outcomes in the WHO-ICF model: Establishment of the upper limb prosthetic outcome measures group," *J. Prosthetics Orthotics*, vol. 21, no. 2, pp. 115–119, Apr. 2009.

[34] W. Hill, P. Kyberd, L. N. Hermansson, S. Hubbard, Ö. Stavdahl, and S. Swanson, "Upper limb prosthetic outcome measures (ULPOM): A working group and their findings," *J. Prosthetics Orthotics*, vol. 21, no. 9, pp. 69–82, Oct. 2009.

[35] C. M. Light, P. H. Chappell, and P. J. Kyberd, "Establishing a standardized clinical assessment tool of pathologic and prosthetic hand function: Normative data, reliability, and validity," *Arch. Phys. Med. Rehabil.*, vol. 83, no. 6, pp. 776–783, Jun. 2002.

[36] S. A. Dalley, D. A. Bennett, and M. Goldfarb, "Functional assessment of the vanderbilt multigrasp myoelectric hand: A continuing case study," in *Proc. Annu. Int. Conf. IEEE Eng. Med. Biol. Soc. (EMBC)*, Chicago, IL, USA, Aug. 2014, pp. 6195–6198.